

## Phosphorylation of BECLIN-1 by BCR-ABL suppresses autophagy in chronic myeloid leukemia

Chuanjiang Yu,<sup>1</sup> Sivahari P. Gorantla,<sup>1</sup> Alina Müller-Rudorf,<sup>1,2</sup> Tony A. Müller,<sup>1</sup> Stefanie Kreutmair,<sup>1</sup> Corinna Albers,<sup>3</sup> Lena Jakob,<sup>1</sup> Lena J. Lippert,<sup>1</sup> Zhenyu Yue,<sup>4</sup> Monika Engelhardt,<sup>1</sup> Marie Follo,<sup>1</sup> Robert Zeiser,<sup>1,2</sup> Tobias B. Huber,<sup>5,6,7</sup> Justus Duyster<sup>4,2</sup> and Anna L. Illert<sup>1,2</sup>

<sup>1</sup>Department of Internal Medicine I, Medical Center, Faculty of Medicine, University of Freiburg, Freiburg, Germany; <sup>2</sup>German Cancer Consortium (DKTK) and German Cancer Research Center (DKFZ), Heidelberg, Germany; <sup>3</sup>Department of Medicine, Klinikum rechts der Isar, Technical University München, München, Germany; <sup>4</sup>Department of Neurology and Neuroscience, Friedman Brain Institute, Mount Sinai School of Medicine, New York, NY, USA; <sup>5</sup>Department of Medicine, University Medical Center Hamburg-Eppendorf, Hamburg, Germany; <sup>6</sup>Department of Medicine, Medical Center, Faculty of Medicine, University of Freiburg, Freiburg, Germany and <sup>7</sup>BIOS Center for Biological Signalling Studies and Center for Systems Biology (ZBSA), Albert-Ludwigs-University, Freiburg, Germany

©2020 Ferrata Storti Foundation. This is an open-access paper. doi:10.3324/haematol.2018.212027

Received: January 18, 2019.

Accepted: August 7, 2019.

Pre-published: August 8, 2019.

Correspondence: ANNA LENA ILLERT - lena.illert@uniklinik-freiburg.de

---

## **Supplemental Methods**

### **Reagents**

Recombinant murine IL-3 (mIL-3), IL-6 (mIL-6), and SCF (mSCF) were purchased from PeproTech. BCR-ABL and ABL were detected by immunoblotting using an ABL-specific antibody 8E9 (BD Biosciences),  $\beta$ -actin antibody and Flag antibody for immunoblotting were from Sigma-Aldrich (AC-15). Tyrosine phosphorylation was detected using a mixture of monoclonal anti-phosphotyrosine 4G10 (Millipore) and PY20 (BD Biosciences). Mouse Beclin-1 antibody was from Novus Biology. Rabbit Beclin-1 antibody, UVRAG antibody, VPS34 antibody, Rubicon antibody and LC3 antibody were purchased from Cell Signaling Technology. ATG14 antibody was from MBL International. Anti-mouse Beclin-1 antibody and anti-rabbit Beclin-1 antibody for immunoprecipitation were from Santa Cruz Biotechnology. Anti-rabbit Flag antibody for immunoprecipitation and VPS15 antibody were purchased from Thermo Scientific. Nilotinib, sorafenib and TAE684 were purchased from Selleckchem and used with a concentration of 2  $\mu$ M for 4 hours. Glutathione S transferase, protein A and protein G beads were from GE Healthcare Life Sciences. Propidium iodide and Flag Affinity Gels were purchased from Sigma-Aldrich. Alexa Fluor® dyes were from Molecular Probes. Rapamycin was purchased from Sigma and used with a concentration of 1  $\mu$ M for 6 hours.

### **Cell culture**

The IL-3–dependent mouse pro-B-cell line Ba/F3 (DSMZ) was cultured in RPMI 1640 (Life technologies) supplemented with 10% FCS (PAA Laboratories), 2 ng/mL IL-3, and penicillin/streptomycin. The human K562 cell line expressing BCR-ABL (DSMZ) was cultured in RPMI 1640 with 10% FCS and penicillin/streptomycin. HEK293 cells, Phoenix E helper virus-free ecotropic packaging cells (G. Nolan, Stanford, CA), NIH/3T3 cells (DSMZ), and *Beclin-1* knockout MEFs were maintained in DMEM (Life technologies) supplemented

with 10% FCS. Cells were cultured in a humidified incubator at 37°C with 5% CO<sub>2</sub>. For starvation, K562 cells were washed twice with PBS and then cultured in 1640 medium without FCS overnight.

### **Expression vectors**

The BCR-ABL miR30-based shRNA vector system was used as described previously.<sup>1</sup> Oligonucleotide sequences of Beclin-1 miR are: Bec-miR1: TGCTGTTGACAGTGAGCGCCCGACTTGTTCCCTATGGAAATAGTGAAGCCACAGATGTATTTCCATAGGGAACAAGTCGGTTCCTACTGCCTCGGA; Bec-miR2: TGCTGTTGACAGTGAGCGCCAGGATGATGTCTACAGAAATAGTGAAGCCACAGATGTATTTCTGTAGACATCATCCTGGATGCCTACTGCCTCGGA. pBABE-puro mCherry-EGFP-LC3B was a kind gift from Jayanta Debnath (Addgene plasmid # 22418). pcDNA4-Beclin-1 (FL) was a kind gift from Qing Zhong (Addgene plasmid # 24388). Beclin-1 tyrosine mutants were generated by the QuickChange mutagenesis kit (Stratagene, Heidelberg, Germany) according to the manufacturer's instructions. For GST-Beclin-1 cloning, Beclin-1 fragments were amplified from pcDNA4-Beclin-1 by PCR and inserted into pGEX-4T2 vector. For retroviral expression, Beclin-1, Beclin-1 Y233E/Y352E and Beclin-1 Y233F/Y352F were subcloned into MSCV-IRES-Berry vector. All constructs were confirmed by sequencing. Details on other constructs and vectors (e.g. Mig BCR-ABL IRES CRE-EGFP, BCR-fragments) are available from the authors upon request.

### **Flow cytometry and cell cycle/ apoptosis staining**

FACS staining was performed as previously described.<sup>1-4</sup> Cell cycle analysis was performed using Click-iT™ EdU Alexa Fluor™ 647 Flow Cytometry Kit (Thermo Scientific) and apoptosis staining using Annexin V Apoptosis Detection Kit PE (eBioscience), both according to the manufacturers instructions.

### **LC3 puncta measurement**

Cells were fixed with 4 % paraformaldehyde and stained with LC3 antibody. Images were collected using Leica TCS SP5 confocal microscope. To quantify LC3 puncta, indicated cells were plated into the Ibidi chamber staining with cell tracker (Thermo Fisher Scientific). Olympus ScanR Screening Station was used for measurement and analysis according to the manufacturer's instructions.

### **Proliferation and clonal growth assays**

Ba/F3 cells expressing indicated constructs ( $1 \times 10^4$ /well) were plated into 96-well plates. At the indicated time, cell viability was measured using the CellTiter96 Proliferation Assay (Promega, Mannheim, Germany) according to the manufacturer's instructions. To analyze clonal growth, retrovirally transduced BM cells were resuspended in HBSS in a concentration of  $1-4 \times 10^4$  cells containing  $2 \times 10^3$  EGFP<sup>+</sup> cells per 100  $\mu$ l and mixed with 1.8 mL of MethoCult 4230 (StemCell Technologies). 1,000 EGFP<sup>+</sup> BM cells in 1 mL of methylcellulose medium were plated in duplicates in 12-well plates and colonies were photographed and counted on day 10.

### **Transduction of murine bone marrow and syngeneic transplantation model**

Balb/c mice were purchased from Charles River, *Atg5* knockout mice were described previously.<sup>5, 6</sup> Murine BM derived cells (BMDCs) were collected after 5-FU treatment. For Beclin-1 knockdown transplantation, BMDCs were infected with retrovirus encoding for BCR-ABL oncogene and a Beclin-1 specific miRs in a vector described previously.<sup>1</sup> *Atg5* knockout BMDCs were infected with retrovirus encoding for BCR-ABL and Cre recombinase (MSCV BA<sup>p185</sup>IRESCreEGFP). After BMDC infection, 5,000 EGFP-positive cells were transplanted together with 195,000 EGFP-negative cells into lethally irradiated female recipient mice. Animals that received a transplant were monitored for signs of disease



development by serial measurement of peripheral blood (PB) counts.

### Supplemental figure legends

**Figure S1. Mice transplanted with pMmiRCtrl–BCR-ABL and pMmiRBec–BCR-ABL showed a comparable immunophenotype in the course of disease.** (A) Cell cycle analysis indicating no differences in cell cycle rate between Beclin-1 miR and control group. n.s., not significant. (B-D) FACS analyses of CD45-positive (B) peripheral blood (PB), (C) bone marrow (BM) and (D) spleen cells of one representative mouse per group for lineage staining with anti-B220, anti-Gr-1 and anti-CD11b confirming the myeloproliferative character of the BCR-ABL-induced disease independent of Beclin-1 downregulation. (E) 5-FU enriched BMDCs from *Atg5<sup>wt/wt</sup>* and *Atg5<sup>flox/flox</sup>* mice were infected with MiG-BCR-ABL-CRE-EGFP and transplanted into lethally irradiated recipient mice. Kaplan-Meier survival curve revealed no differences in the *Atg5* control and deleted group. (F) Mice were analyzed for leukemia induction and progression by white blood cell (WBC) measurement at the indicated days. (G) PCR analyses of genomic DNA from splenocytes of diseased mice exhibit correct *Atg5* deletion upon Cre expression.

**Figure S2. Beclin-1 downregulation does not influence hematopoietic cells with a murine BM transplantation model.** Mice transplanted with bone marrow cells infected with sole Beclin-1 miR3 construct showed normal (A) survival rate, (B) WBC amount, (C) RBC amount, (D-G) percentage of lineage markers (anti-CD45, anti-B220, anti-Gr-1, anti-Thy1.2 and anti-CD11b) compared to mice transplanted with control miR construct. n.s., not significant, Student's t test.

**Figure S3. BCR-ABL activity inhibits autophagy by Beclin-1 complex alternation.** (A) Immunoblot analyses reveal nilotinib-induced autophagy in K562 cells seen by accumulation

of autophagosome-associated LC3-II and **(B)** increased LC3-puncta formation. mCherry-EGFP-LC3-transduced K562 cells were treated for 12 h +/- 2  $\mu$ M nilotinib, fixed, stained (anti-LC3-antibody) and DAPI-counterstained. Scale bar 10  $\mu$ m. **(C)** LC3-puncta quantitation via OlympusScanR station (3.2 vs. 18.5 dots/cell); \*\*\*\* $p < 0.0001$  by Student's t-test. **(D)** LC3-II expression and **(E)** LC3-puncta-formation in BCR-ABL-WT- or BCR-ABL-T315I mutant-expressing Ba/F3 cells upon nilotinib treatment. Treatment for 12 h with 2  $\mu$ M nilotinib indicates that selective blockage of active BCR-ABL triggers autophagy by accumulation of LC3-II and LC3-puncta (Scale bar 10  $\mu$ m). **(F)** LC3-puncta quantitation (2.5 vs. 7.7 dots/cell, \*\*\* $p < 0.001$ , 2.4 vs. 6.5 dots/cell, \*\*\* $p < 0.001$ , and 1.7 vs. 2.2 dots/cell, n. s., not significant). **(G)** BCR-ABL inhibition alters recruitment of Beclin-1 binding partners to the Beclin-1 complex. Co-Immunoprecipitation of indicated proteins (ATG14, UVRAG, VPS34, VPS15 and Rubicon) with Beclin-1 in K562 cells with/without nilotinib treatment shows that BCR-ABL inhibition leads to altered recruitment of positive and negative regulators. Quantitation was normalized to Beclin-1 IP-levels.

**Figure S4. Phosphorylation of Beclin-1 in CML patients and alters the Beclin-1 complex composition.**

**(A)** Co-localization of BCR-ABL and Beclin-1 in K562 cells. BCR (red), Beclin-1 (green), DAPI (blue); Scale bar 10 $\mu$ m. **(B)** Primary mononuclear cells of PB (PBMCs) from BCR-ABL<sup>+</sup> CML patients at initial diagnosis show phosphorylated Beclin-1 levels compared to healthy control WBCs. Beclin-1 was immunoprecipitated and immunoblotted with phosphotyrosine antibody. **(C)** Quantitation of immunoprecipitation of FLAG-tagged phosphorylation-deficient Beclin-1 Y233F/Y352F mutant (BecFF) in K562 cells normalized to Beclin-1 (n=3) (Figure 4E). Bars represent mean $\pm$ SD. \* $p < 0.05$ , \*\* $p < 0.01$ , Student's t test.

**Figure S5. BCR-ABL-mediated Beclin-1 phosphorylation alters the stability of Beclin-1**

**complex components, but does not influence starvation-induced autophagy.** (A) Immunoprecipitation of FLAG-tagged phosphorylation-deficient Beclin-1 Y233E/Y352E mutant (BecFF) in Nilotinib-treated K562 cells indicates altered autophagy complex formation compared to the phosphorylation-deficient Beclin-1 mutant (BecFF) and Beclin-1 WT. (B) LC3 puncta was measured by confocal microscopy in K562 cells transduced with mCherry-EGFP-LC3 upon starvation. Scale bar, 10  $\mu$ m. (C) Quantitation of LC3 puncta in K562 cells with and without starvation via Olympus ScanR screening station (4.8 vs. 11.9 dots/cell,  $p < 0.01$ ). Bars represents mean  $\pm$  SD.  $**p < 0.01$  by Student's t test. (D) LC3 expression levels were detected in K562 cells with and without starvation. (E) LC3 expression levels were detected in K562 cells transduced with the indicated Beclin-1 construct after starvation. (F) LC3 puncta was measured by confocal microscopy in K562 cells transduced with mCherry-EGFP-LC3 and the indicated Beclin-1 construct upon starvation. Scale bar, 10  $\mu$ m. (G) Quantitation of LC3 puncta in K562 cells transduced with mCherry-EGFP-LC3 and the indicated Beclin-1 construct upon starvation using an Olympus ScanR screening station (9.5, 15.8, 14.8, and 16.5 dots/cell, respectively;  $**p < 0.01$  for comparison of Beclin-1 WT, Beclin-1 EE, and Beclin-1 FF to empty vector, Student's t test). Bars represent mean  $\pm$  SD. (H) LC3 expression levels in K562 cells expressing Beclin-1 EE or Beclin-1 FF treated with 1  $\mu$ M Rapamycin or DMSO (control).

### Supplemental References

1. Albers C, Illert AL, Miething C, et al. An RNAi-based system for loss-of-function analysis identifies Raf1 as a crucial mediator of BCR-ABL-driven leukemogenesis. *Blood*. 2011;118(8):2200-2210.
2. Muller TA, Grundler R, Istvanffy R, et al. Lineage-specific STAT5 target gene activation in hematopoietic progenitor cells predicts the FLT3(+)-mediated leukemic phenotype. *Leukemia*. 2016;30(8):1725-1733.
3. Illert AL, Albers C, Kreutmair S, et al. Grb10 is involved in BCR-ABL-positive leukemia in mice. *Leukemia*. 2015;29(4):858-868.
4. Klein C, Zwick A, Kissel S, et al. Ptch2 loss drives myeloproliferation and myeloproliferative neoplasm progression. *The Journal of experimental medicine*. 2016;213(2):273-290.
5. Hara T, Nakamura K, Matsui M, et al. Suppression of basal autophagy in neural cells causes neurodegenerative disease in mice. *Nature*. 2006;441(7095):885-889.
6. Liu S, Hartleben B, Kretz O, et al. Autophagy plays a critical role in kidney tubule maintenance, aging and ischemia-reperfusion injury. *Autophagy*. 2012;8(5):826-837.

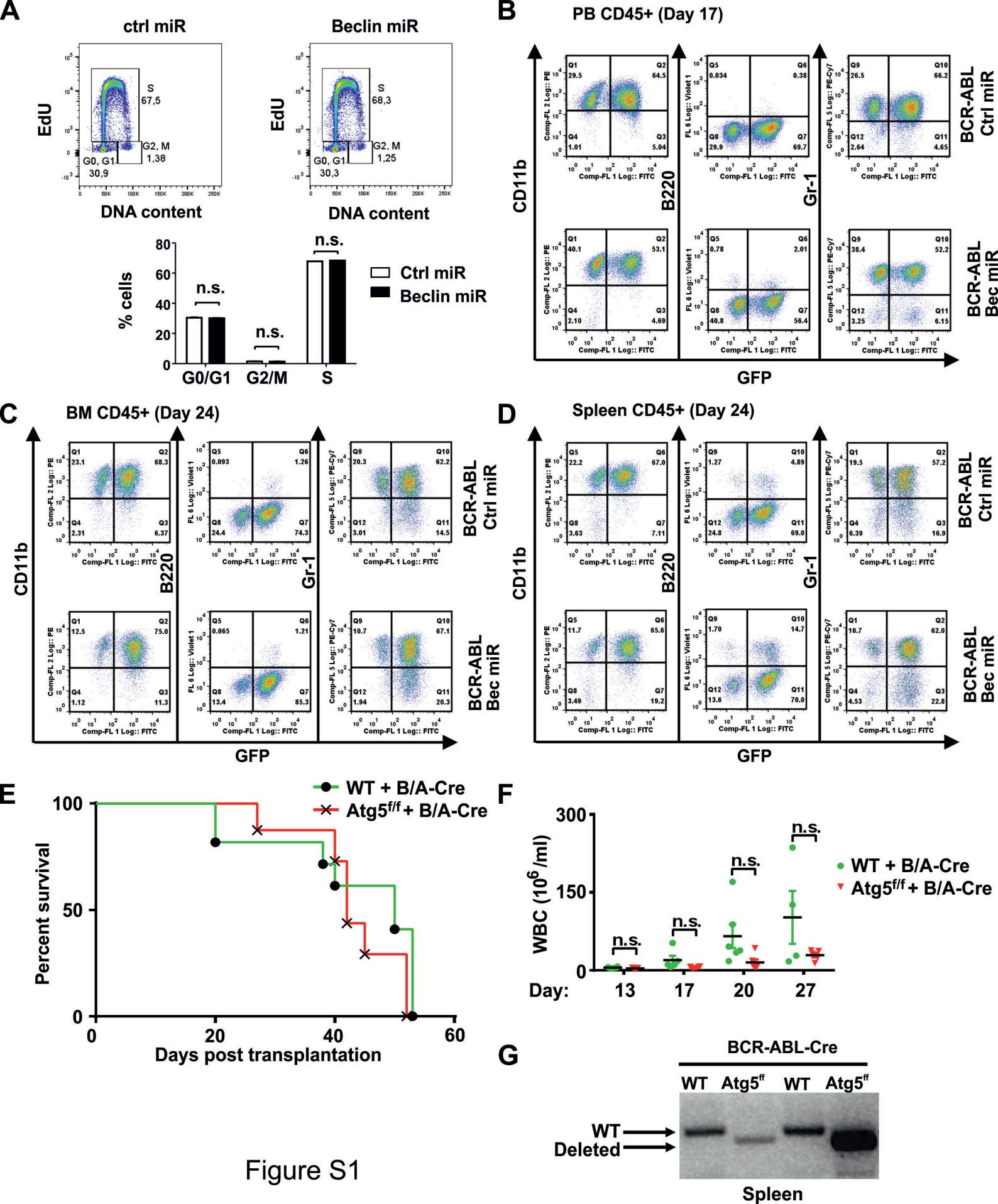


Figure S1

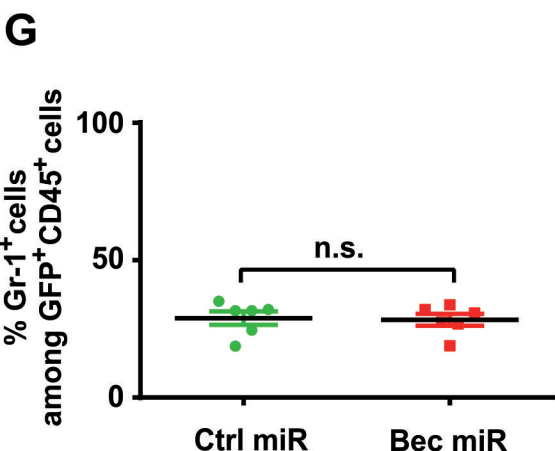
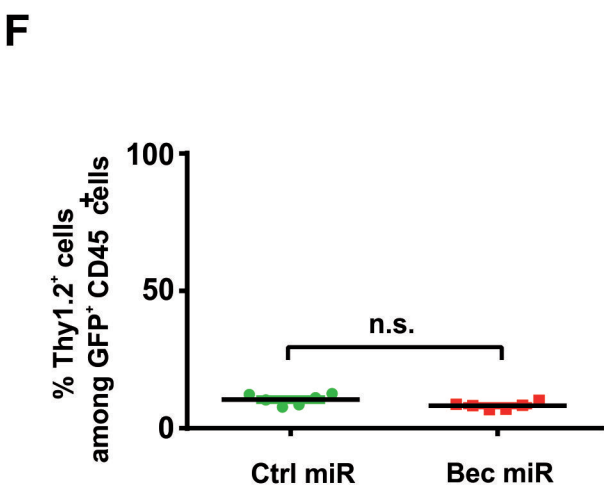
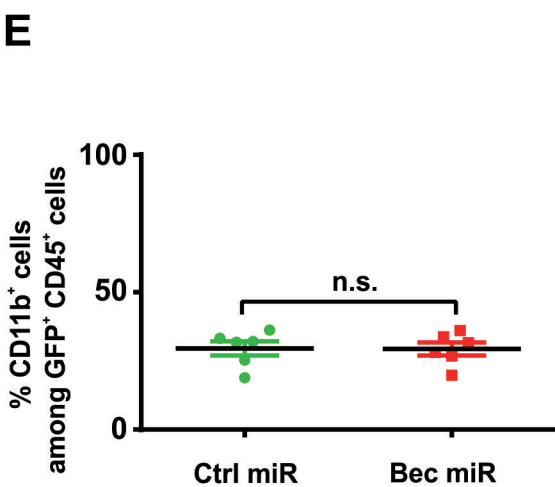
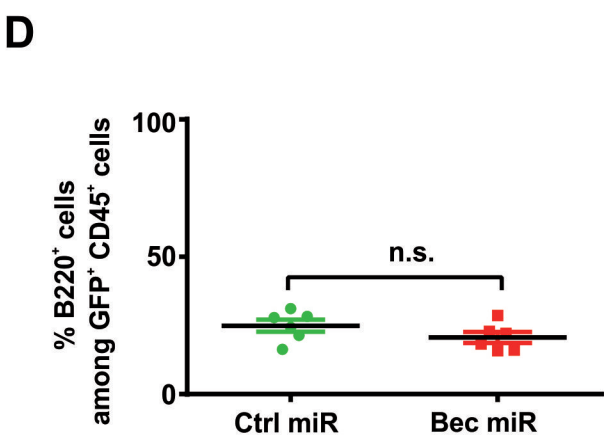
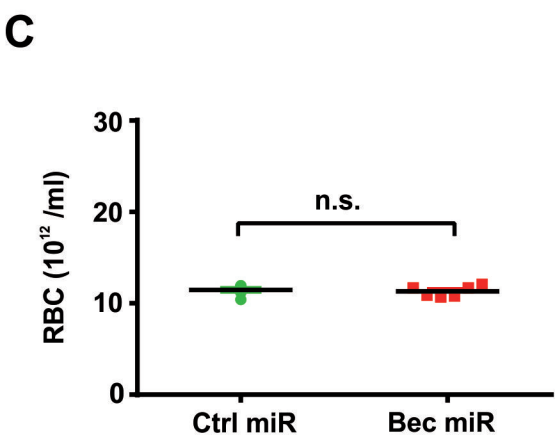
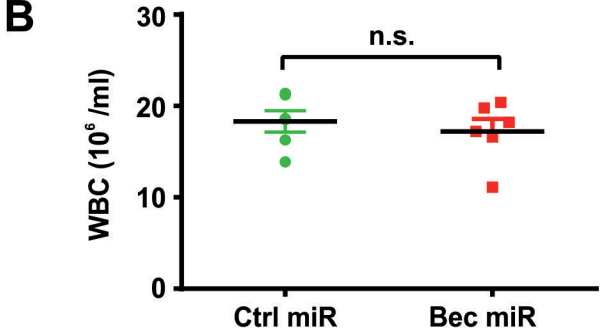
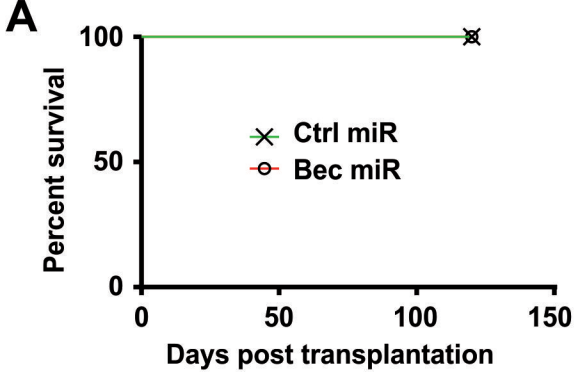


Figure S2

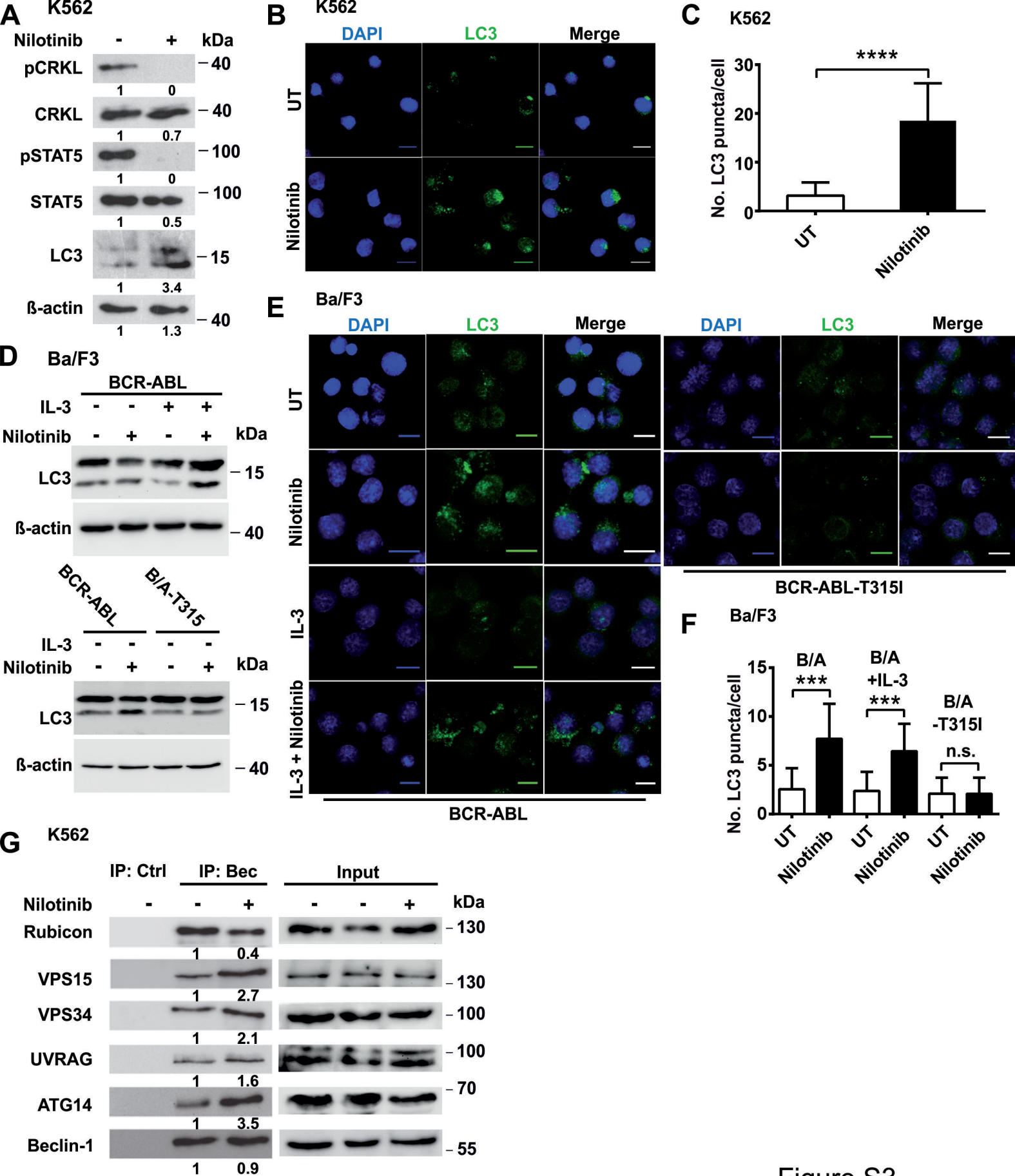


Figure S3



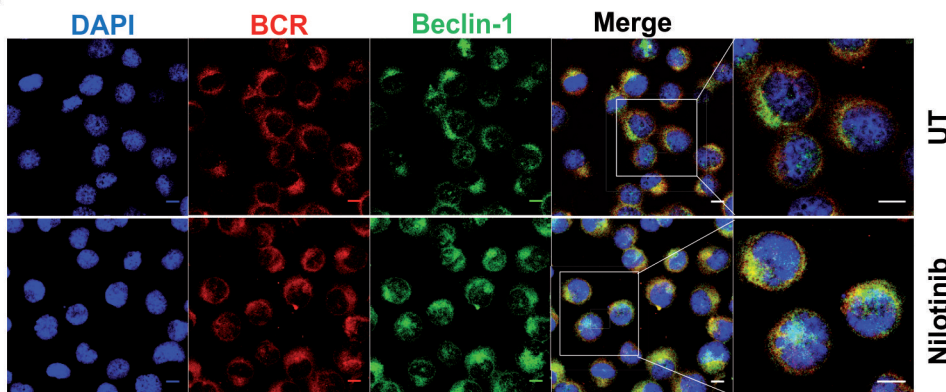
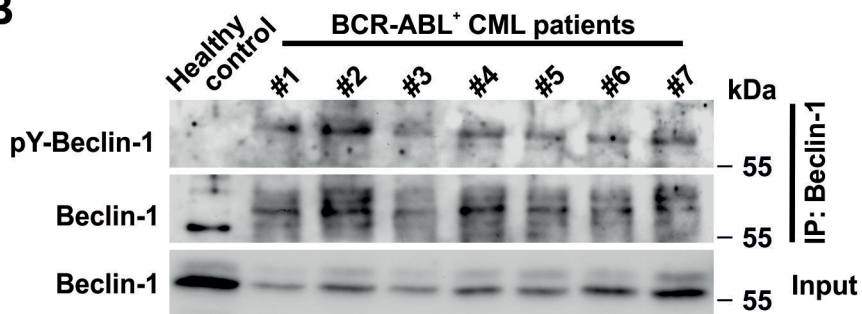
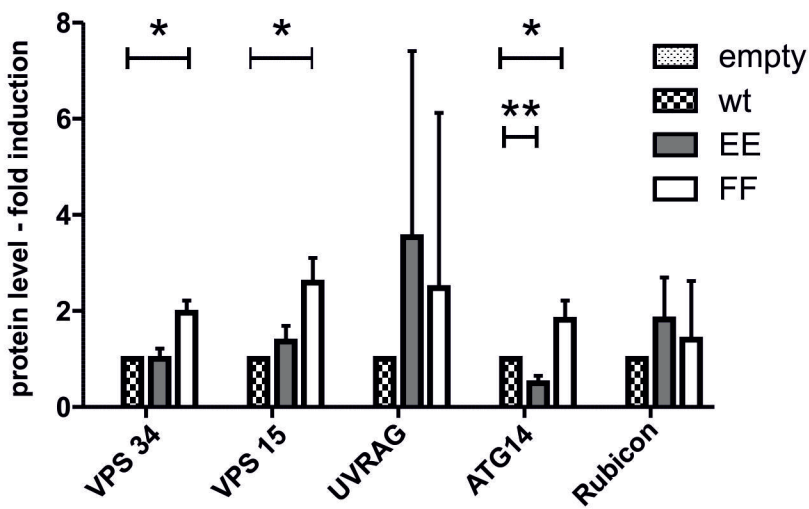
**A****B****C**

Figure S4

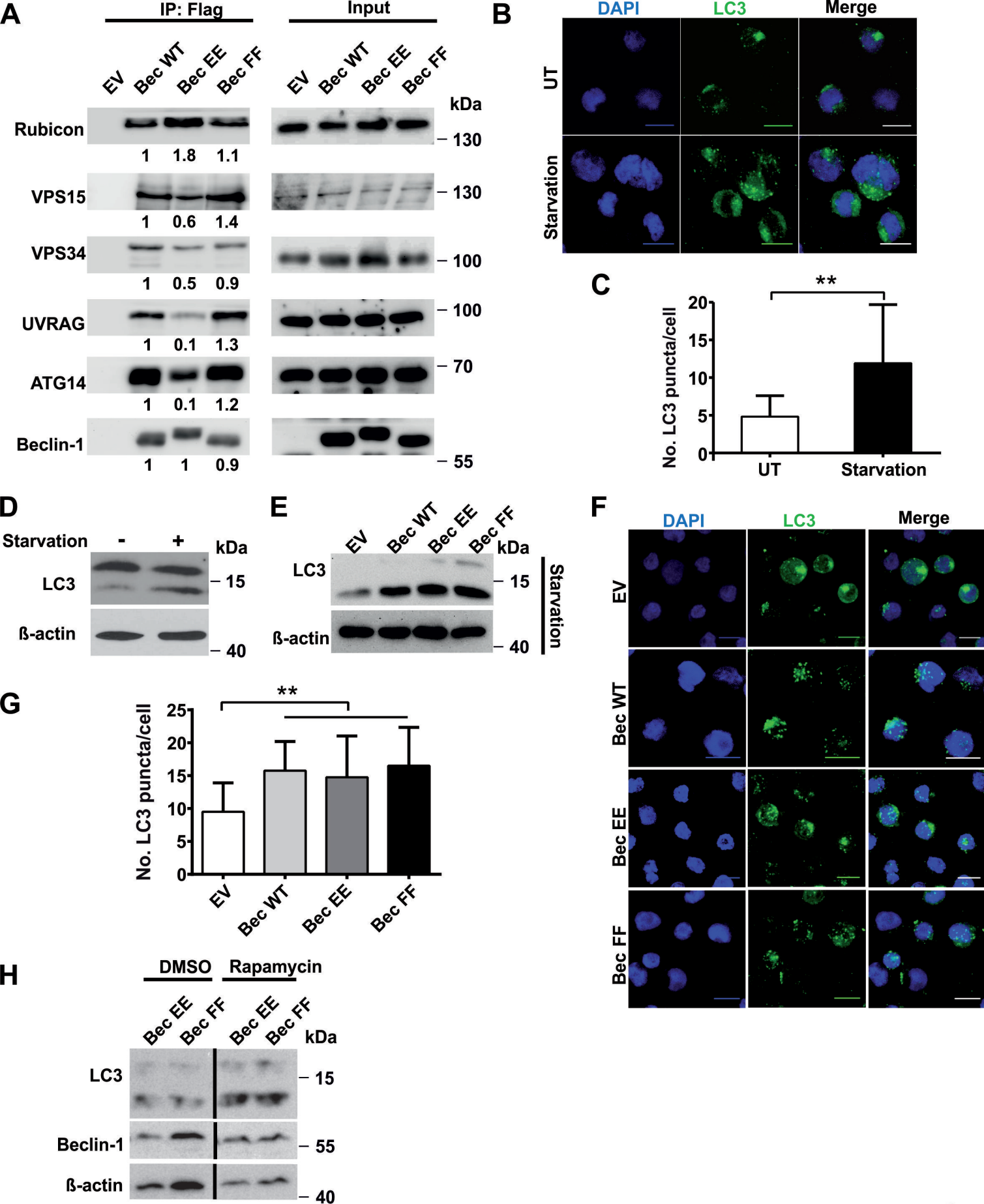


Figure S5